Secondary Instability in Plane Channel Flow with Spatially Periodic Perturbations

Michael F. Schatz[a] and Harry L. Swinney[b]

Center for Nonlinear Dynamics and Department of Physics, The University of Texas, Austin, Texas 78712

(Received 20 April 1992)

Laboratory experiments on plane channel flow with a streamwise-periodic array of cylinders reveal a bifurcation from two-dimensional traveling waves to three-dimensional spanwise standing waves. The standing waves select a wave number that is independent of the wave number imposed initially by time-periodic disturbances. The stable tertiary flow stands in contrast with most open flows where instability develops directly to turbulence.

PACS numbers: 47.20.Ky, 47.20.Ft, 47.35.+i, 47.60.+i

The onset of three-dimensional motion is an important stage in the transition to turbulence for open flows, where fluid advects through the system [1,2]. Typically, three-dimensional behavior grows from two-dimensional waves that arise from the primary instability [3], but distinguishing separate stages is difficult because open flows generally do not equilibrate at finite amplitude after each instability. Instead, successive instabilities lead directly to turbulence as the flow develops downstream [4]. However, states that are stable for a range of control parameter (e.g., Reynolds number R) have been recently found in open flows that contain spatially periodic geometric perturbations [5–7]. A laboratory experiment and numerical simulation on a spatially perturbed plane channel demonstrated that the primary instability can occur as a supercritical (continuous) Hopf bifurcation to stable two-dimensional traveling waves [7]. A supercritical primary transition often occurs in closed flows, where fluid never advects out of the system (e.g., Couette-Taylor flow or Rayleigh-Bénard convection). In contrast to most open flows, a sequence of well-separated transitions in closed flows lead to ordered (nonturbulent) states beyond the primary instability.

In this Letter we present evidence from laboratory experiments for a secondary transition leading to a stable ordered state in the open flow through a spatially perturbed plane channel. Our results suggest that open flows can exhibit a sequence of bifurcations to stable nonturbulent states. Such behavior is particularly interesting since instability in the spatially perturbed plane channel, like that in most flows where fluid passes across system boundaries, is *convective* [8] (disturbances grow in time only in a comoving reference frame) rather than *absolute* (disturbances grow in any frame) [7]; previous work has shown the distinction between convective and absolute instabilities is crucial in characterizing transition phenomena in fluids and plasmas [9–13].

Figure 1 depicts a plane channel flow that is geometrically perturbed by cylinders in a spatially periodic array. The Reynolds number is defined as $R=U_0h/\nu$ with the kinematic viscosity ν, channel half-depth h, and velocity scale U_0, where U_0 is defined as $\frac{3}{2}$ times the streamwise velocity u averaged across y. U_0 and h are used to scale velocity, length, and time (h/U_0).

The experiment is performed in a water channel with $h=0.794$ cm and with 21 cylinders approximating an infinite periodic array. Cylinder 1 (numbering from upstream to downstream) lies a distance of 160 downstream from the channel inlet; the unperturbed flow approaches a parabolic profile in a length $D\approx 0.11U_0h/\nu < 20$ for the range of R investigated [14]. The experiment maintains constant mass flux inflow-outflow boundary conditions in x. The fluid temperature is controlled to $\pm 0.1\,^{\circ}$C and the upstream root-mean-square velocity fluctuation (noise) is typically 0.07% of U_0.

Three-dimensional time-periodic disturbances [15] are imposed by an oscillating paddle, whose axis of rotation is located at ($x=-4.8$, $y=0$) upstream of cylinder 1 (Fig. 1). The range of oscillation frequencies investigated lies within $\pm 5\%$ of the natural frequency selected by the traveling-wave state [7]. Magnetically mounted bumps with a semicircular cross section (radius 0.5) are placed at regular intervals along z on one side of the paddle. The presence of the bumps imposes a three-dimensional variation whose wave number k_1 can be controlled by varying the number of bumps and their center-to-center spacing.

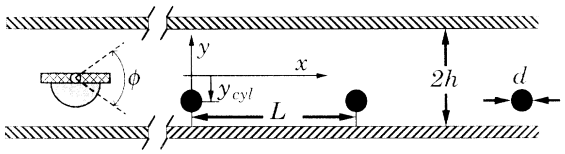

FIG. 1. Our geometry of plane channel flow with spatially periodic perturbations is defined in units of the half-depth h by the cylinder spacing $L=6.66$, cross-channel location $y_{cyl}=-0.50$, and the cylinder diameter $d=0.40$. Flow is in the streamwise direction x, and the spanwise dimension z (perpendicular to the figure) and ranges from -20 to 20 in the experiment. At the inlet of the cylinder array, time-periodic disturbances are imposed by a paddle, which oscillates about the channel center line with an angular displacement $\phi=72°$. Semicircular bumps (shaded) whose length along z is ≈ 1 are placed on the paddle to impose a controlled initial three dimensionality on the disturbance. The paddle and bumps are drawn to scale.

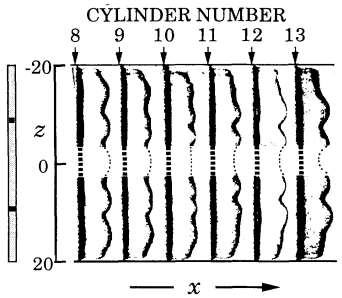

FIG. 2. A digitally enhanced image of the flow at $R=170$ shows the standing-wave state. Dye for each wave front is produced electrochemically at the nearest upstream cylinder; the straight vertical dye lines mark the separation bubble immediately downstream of each cylinder, whose position is indicated by arrows. Each dye wave front is recorded separately in time; however, the temporal periodicity of the flow is used to show all dye fronts at the same phase in this composite image. Near $z=0$, channel wall braces block a direct view of the flow; thus, dotted lines have been drawn in to guide the eye. An initial three dimensionality is imposed by two bumps on the disturbance paddle, which is shown approximately to scale at the far left; the center-to-center spacing of the bumps imposes an initial wave number $k_i=0.42$. The standing-wave pattern is *not* advected downstream—see text.

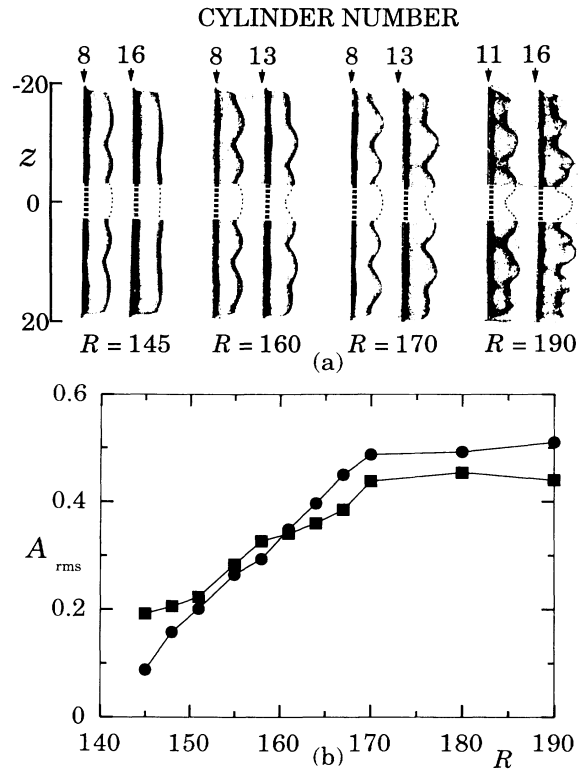

FIG. 3. (a) Local maxima of standing-wave amplitude are compared simultaneously between upstream and downstream regions for different Reynolds numbers. The disturbance paddle imposes an initial wave number $k_i=0.9$. (b) Standing-wave amplitude $A_{\rm rms}$ vs R is plotted for comparison between upstream (■) and downstream (●) locations in the experiment. Each data point represents the average of seven dye fronts; the error bars for each data point are smaller than the symbol size. The disturbance paddle imposes an initial wave number $k_i=0.42$.

Flow visualization reveals that the time-periodic disturbances evolve to standing waves along the span z (Fig. 2). With thymol blue, a pH indicator, dissolved in the working fluid, dye is produced electrochemically near the cylinders, which serve as electrodes, and is gathered into fronts by the flow field [16]. Digital imaging methods are used to acquire, enhance, and analyze video images of the dye fronts. Between cylinders 8 and 9, the dye front displays a nearly sinusoidal variation along z. This variation decreases between cylinders 10 and 11 and the dye front becomes nearly two dimensional (independent of z). Between cylinders 13 and 14, the spanwise wave reappears strongly; however, the phase along z has shifted by 180° relative to the dye front between cylinders 8 and 9; for example, an upstream dye front "peak," which leads the mean streamwise position of the front, becomes a downstream dye front "valley," which lags the mean front position. (The amplitude pinching of the peaks between cylinders 9 and 10 indicates the eventual location of the valleys.) Downstream of the region shown in Fig. 2, the dye fronts become nearly two dimensional again between cylinders 16 and 17, and then a spanwise wave, whose phase matches that shown between cylinders 8 and 9, emerges between cylinders 18 and 19.

The onset of the spanwise standing waves occurs at $R_2\approx 160$ (Fig. 3). The standing waves develop spatially in the streamwise direction because they bifurcate from convectively unstable two-dimensional traveling waves. Growth or decay of the secondary instability is estimated by comparing local maxima of dye front distortion at different streamwise positions (for example, in Fig. 2 the dye front between cylinders 8 and 9 is compared to the dye front between cylinders 13 and 14). For lower values of R [e.g., $R=145$ in Fig. 3(a)], three-dimensional disturbances observed upstream decay downstream to the two-dimensional basic flow. However, for larger values of R [e.g., $R=190$ in Fig. 3(a)], three-dimensional disturbances grow downstream. The dye front distortion is quantitatively characterized by the root-mean-square fluctuations $A_{\rm rms}$ about the average streamwise position of the dye front, as computed from digitized images of the dye fronts. The "crossover" of $A_{\rm rms}$ between upstream and downstream locations as R is increased occurs at $R_2=160\pm 5$, as can be seen in Fig. 3(b). The instability at R_2 is well above the onset of the primary instability at $R_1=130$ [7]. The downstream amplitudes are presumably nearly saturated, but to demonstrate this would require a channel whose streamwise length would be longer than our present channel. In any event, our results demonstrate that three dimensionality grows slowly over several periods of the two-dimensional traveling

wave [approximately 10 periods separate the upstream and downstream amplitudes in Fig. 3(b)]. In contrast, for other open flows, the progression from onset of three dimensionality to *turbulence* can occur in only a few periods of the two-dimensional traveling wave [2].

Velocity measurements [Fig. 4(a)] in the laboratory frame demonstrate that no additional frequencies accompany the onset of three-dimensional standing waves. Power spectra from single point measurements [Fig. 4(b)] show only the fundamental frequency and harmonics [17]. This suggests that the phase of the standing wave is locked to a given streamwise location in the laboratory frame for fixed R and initial disturbance conditions (paddle frequency, amplitude, k_i). Flow visualization confirms that standing-wave patterns, such as Fig. 2, do not drift downstream, although individual dye fronts are advected downstream in the open flow.

For different k_i, the same characteristic spanwise wave number, $k_z \approx 0.9$, is selected, but the details of the spatial evolution from k_i to k_z depend on k_i. For k_i significantly less than 0.9 ($k_i = 0.31$ and $k_i = 0.42$ in Fig. 5), disturbances evolve directly to $k_z \approx 0.9$. For k_i near 0.9 ($k_i = 0.78$ and $k_i = 1.09$ in Fig. 5), the standing wave maintains the imposed wave number such that $k_i \approx k_z$. For k_i significantly greater than 0.9 ($k_i = 1.4$ in Fig. 5), counterpropagating waves with $k_z \approx 0.9$ move from the span walls at $z = \pm 20$ toward the center; we expect that the counterpropagating waves will evolve to standing waves sufficiently far downstream, although our present channel is too short to confirm this conjecture. Evidence for counterpropagating waves is also seen for $k_i = 0.31$; in this case, a single bump at $z = 0$ on the paddle imposes a localized three dimensionality that is observed to propagate to the span walls and to form the standing wave pictured in Fig. 5 as the flow evolves from upstream to downstream.

No theoretical predictions exist for secondary instability in the geometry of Fig. 1; however, Amon and Patera [6] numerically investigated secondary instability in a plane channel flow where grooves cut in one wall replaced cylinders as streamwise-periodic perturbations. Performing a direct simulation of the (nonlinear) Navier-Stokes equations, they found a stable three-dimensional flow bifurcated from two-dimensional traveling waves; moreover, a phase portrait constructed from velocity time series indicated the three-dimensional flow was periodic in the laboratory frame. However, standing-wave behavior could not be detected in their simulations because the computational domain contained only a single groove with periodic boundary conditions imposed in x.

For open flows with a convective instability, flow structures are "noise sustained" [18]; i.e., no structures are observed in the absence of external noise (disturbances). In such systems it is usually difficult to distinguish between the role of disturbances and the role of the intrinsic dynamics in the formation of structures. This difficulty is particularly acute when the flow develops directly to turbulence. Our work considers an open system with well-controlled external disturbances and simple intrinsic dynamics, and we observe stable disturbance-generated structures past the secondary instability. This system with a stable tertiary flow can serve as a quantitative test for theoretical ideas regarding the onset of secondary instability [3,19,20]. Moreover, since the onset of standing waves is accompanied by the loss of translational symmetry along z, viewing the transition as a symmetry-breaking bifurcation should offer further physical insight [21]. We expect future work on spatially perturbed channel flow to investigate in detail the interplay between dy-

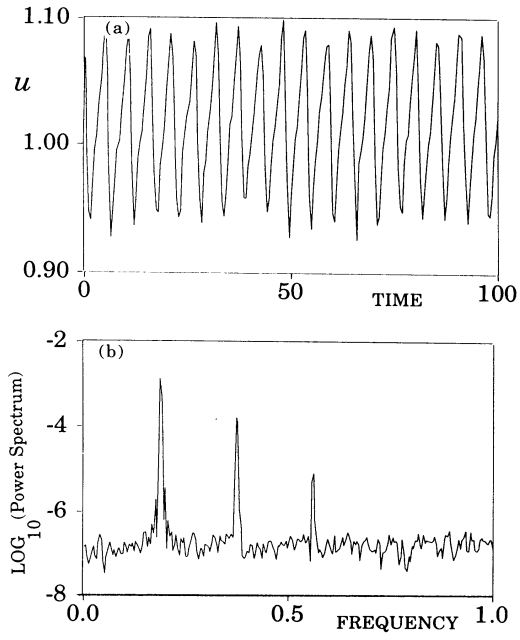

FIG. 4. (a) Time series and (b) power spectrum of the streamwise velocity u measured by laser Doppler velocimetry at $x = 3.9$ downstream of cylinder 18, $y = 0$, and $z = -5.2$ for $R = 170$ and $k_i = 0.42$.

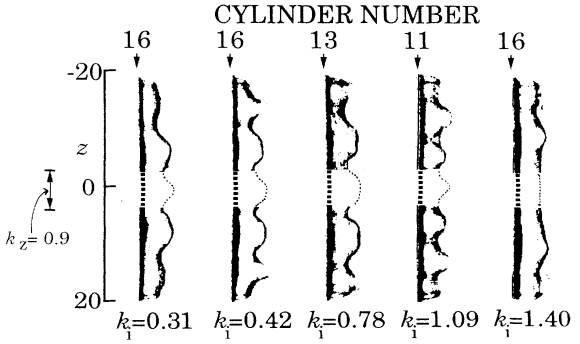

FIG. 5. The selection of a characteristic wave number $k_z \approx 0.9$ by the flow is illustrated for different wave numbers k_i imposed initially on time-periodic disturbances at $R = 190$.

namics and disturbances in convectively unstable open flows.

We thank Randy Tagg and Dwight Barkley for helpful discussions. This work was supported by the Physics Division of the Office of Naval Research.

[a]Electronic address: schatz@chaos.utexas.edu.
[b]Electronic address: swinney@chaos.utexas.edu.

[1] R. T. Pierrehumbert and S. E. Widnall, J. Fluid Mech. **114**, 59 (1982).
[2] T. Herbert, Annu. Rev. Fluid Mech. **20**, 487 (1988).
[3] B. J. Bayly, S. A. Orszag, and T. Herbert, Annu. Rev. Fluid Mech. **20**, 359 (1988).
[4] M. Nishioka and M. Asai, in *Turbulence and Chaotic Phenomena in Fluids,* edited by T. Tatsumi (North-Holland, Amsterdam, 1984), p. 87.
[5] G. E. Karniadakis, B. B. Mikic, and A. T. Patera, J. Fluid Mech. **192**, 365 (1988).
[6] C. H. Amon and A. T. Patera, Phys. Fluids A **1**, 2005 (1989).
[7] M. F. Schatz, R. P. Tagg, H. L. Swinney, P. F. Fischer, and A. T. Patera, Phys. Rev. Lett. **66**, 1579 (1991).
[8] Local absolute instability may exist in the near wake of the cylinders, but the absence of self-sustained oscillations indicates that such regions, if they exist, are small; see, for example, J. M. Chomaz, P. Huerre, and L. G. Redekopp, Phys. Rev. Lett. **60**, 25 (1988).
[9] A. Bers, in *Basic Plasma Physics I,* edited by A. A. Galeev and R. N. Sudan (North-Holland, New York, 1983), Chap. 3.
[10] P. Huerre and P. A. Monkewitz, Annu. Rev. Fluid Mech. **22**, 473 (1990).
[11] R. Tagg, W. S. Edwards, and H. L. Swinney, Phys. Rev. A **42**, 831 (1990).
[12] K. L. Babcock, G. Ahlers, and D. S. Cannell, Phys. Rev. Lett. **67**, 3388 (1991).
[13] A. Tsameret and V. Steinberg, Phys. Rev. Lett. **67**, 3392 (1991).
[14] H. Schlichting, *Boundary Layer Theory* (McGraw-Hill, New York, 1968), 6th ed.
[15] Controlled disturbances have long been used to study transition in convectively unstable open flows; see, for example, G. B. Schubauer and H. K. Skramstad, J. Res. Natl. Bur. Stand. **38**, 251 (1947); P. S. Klebanoff, K. D. Tidstrom, and L. M. Sargent, J. Fluid Mech. **12**, 1 (1962).
[16] W. Merzkirch, *Flow Visualization* (Academic, Orlando, 1987).
[17] Similar spectra have been observed at the appearance of three dimensionality in other open flows; see, for example, Y. S. Kachanov, V. V. Kozlov, V. Y. Levchenko, and M. P. Ramazanov, in *Laminar-Turbulent Transition,* edited by V. V. Kozlov (Springer, Berlin, 1985), p. 61.
[18] R. J. Deissler, J. Stat. Phys. **40**, 371 (1985).
[19] R. T. Pierrehumbert, Phys. Rev. Lett. **57**, 2157 (1986).
[20] M. J. Landman and P. G. Saffman, Phys. Fluids **30**, 2339 (1987).
[21] J. D. Crawford and E. Knobloch, Annu. Rev. Fluid Mech. **23**, 341 (1991).

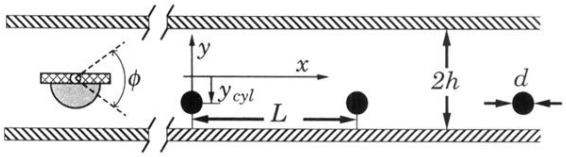

FIG. 1. Our geometry of plane channel flow with spatially periodic perturbations is defined in units of the half-depth h by the cylinder spacing $L=6.66$, cross-channel location $y_{cyl}=-0.50$, and the cylinder diameter $d=0.40$. Flow is in the streamwise direction x, and the spanwise dimension z (perpendicular to the figure) and ranges from -20 to 20 in the experiment. At the inlet of the cylinder array, time-periodic disturbances are imposed by a paddle, which oscillates about the channel center line with an angular displacement $\phi=72°$. Semicircular bumps (shaded) whose length along z is ≈ 1 are placed on the paddle to impose a controlled initial three dimensionality on the disturbance. The paddle and bumps are drawn to scale.